UPF3B modulates endoplasmic reticulum stress through interaction with inositol-requiring enzyme-1α

Jikai Wen (jkwen@scau.edu.cn)
South China Agricultural University https://orcid.org/0000-0002-4010-4416
Xingsheng Sun
South China Agricultural University
Ruqin Lin
South China Agricultural University
Xueying Qi
South China Agricultural University
Xinxia Lu
South China Agricultural University
Zhikai Wu
South China Agricultural University
Tianqing Jiang
South China Agricultural University
Jun Jiang
South China Agricultural University
Peiqiang Mu
South China Agricultural University
Qingmei Chen
South China Agricultural University
Yiqun Deng
South China Agricultural University https://orcid.org/0000-0002-6838-3779

Article

Keywords: ER stress, IRE1α, NMD, UPF3B, UPR

Posted Date: December 19th, 2023

DOI: https://doi.org/10.21203/rs.3.rs-3433963/v1

Additional Declarations: There is no duality of interest

Abstract

The unfolded protein response (UPR), as a conserved and adaptive intracellular pathway, relieves the endoplasmic reticulum (ER) stress by activating ER transmembrane stress sensors. As the consequence of ER stress, the inhibition of nonsense mediated mRNA decay (NMD) is due to an increase in the phosphorylation of eIF2α, which has the effect of inhibiting translation. However, the role of NMD in the maintenance of ER homeostasis remains unclear. In this study, we found that the three NMD factors, UPF1, UPF2 or UPF3B, are required to negate UPR. Among these three NMD factors, UPF3B specifically interacts with inositol-requiring enzyme-1α (IRE1α). This interaction inhibited the kinase activity of IRE1α, abolished autophosphorylation and reduced IRE1α clustering for ER stress. BiP and UPF3B jointly control the activation of IRE1α on both sides of the ER membrane. Under stress condition, the phosphorylation of UPF3B was increased and the phosphorylated sites were identified. Both the genetic mutation UPF3B^{Y160D} and the phosphorylation at Thr169 of UPF3B abolished its interaction with IRE1α and UPF2, respectively, led the activation of ER stress and NMD disfunction. Our study reveals a key physiological role for UPF3B in the reciprocal regulatory relationship between NMD and ER stress.

Introduction

The endoplasmic reticulum (ER) is a cellular organelle consisting of a system of membranes that is the site of protein and lipid synthesis and regulates intracellular protein folding and transport [1]. External stimuli disrupt the function of homeostatic factors in the ER, leading to the disruption of protein synthesis and the accumulation of unfolded or misfolded proteins, ultimately leading to ER stress [2, 3].To respond to stress, cells activate an intracellular signaling pathway called the unfolded protein response (UPR) [4, 5]. The UPR is a highly conserved cellular process in all eukaryotes that enhances the protein folding and processing capabilities of the ER and restores ER homeostasis[2, 3, 6]. The UPR consists of three signaling pathways in mammalian cells, PERK-eIF2α, IRE1-XBP1, and ATF6 [7], among which IRE1-XBP1 pathway is the most conserved in eukaryotes [8, 9]. In cells, both newly synthesized and pre-existing proteins are under constant threat of misfolding. The accumulation of damaged proteins disrupts intracellular homeostasis, leading to pathological conditions and even cell death [10]. Upon ER stress activation, BiP (also known as GRP78), as an ER-resident master regulator protein, dissociates from three key ER transmembrane stress sensors to be activated [11, 12]. As a result, high levels of UPR such as IRE1/XBP1s, PERK/ATF4 and ATF6, regulate the expression and activation of ER stress-related pro-apoptotic proteins, such as CHOP and caspase-12, and pro-survival molecules, such as GADD34 and BiP, which ultimately determine whether cells undergo apoptosis or adapt to the stress condition [13, 14, 15].

Nonsense-mediated mRNA decay (NMD) is a quality control pathway that degrades transcripts carrying premature translation termination codons [16, 17]. As a conserved translation-coupled mRNA quality control mechanism in eukaryotes [18], NMD is estimated to regulate the stability of approximately 5–10% of normal physiological mRNAs [19, 20]. However, the physiological significance of NMD and NMD factors remains unclear. The most conserved NMD factors are the up-frameshift (UPF) proteins UPF1, UPF2 and

UPF3 (UPF3B in mammalian cells). The human NMD machinery consists of additional morphogenetic suppressors of genitalia (SMG) proteins, including SMG 1, 5, 6, 7, 8 and 9 [21, 22]. ER stress has been reported to inhibit NMD [23]. Activation of PERK inhibits NMD, possibly due to high phosphorylation of eIF2α [23]. However, the mechanistic role of NMD, in particular UPF1, UPF2 and UPF3B in ER stress, remains unclear.

In this study, we first demonstrated that knockdown of any of the NMD factors, UPF1, UPF2 and UPF3B, activates ER stress and leads to cell apoptosis. Among the three key NMD factors, UPF3B showed a unique regulatory role in inhibiting the activation of IRE1α. When overexpressed, UPF3B interacts with IRE1α and binds directly to its kinase domain. This interaction inhibits the phosphorylation and oligomerization of IRE1α and subsequently attenuates the extent of ER stress. BiP and UPF3B jointly control the activation of IRE1α on both sides of the ER membrane, as overexpression of BiP inhibits IRE1α phosphorylation to base levels in UPF3B-depleted cells, and overexpression of UPF3B also effectively reduces IRE1α phosphorylation in BiP knockdown cells. In addition, overexpression of UPF2 competes with UPF3B to inhibit the interaction between IRE1α and UPF3B. Under stress stimuli with tunicamycin (Tm) or thapsigargin (Tg) treatment, UPF3B was apparently phosphorylated. Phosphorylation of UPF3B at threonine 169 under stress, similar to the genetic mutation UPF3B^{Y160D} that causes X-linked mental retardation [24], attenuates its interaction with IRE1α and UPF2, respectively, and fails to rescue the apoptosis caused by UPF3B depletion. This suggests that phosphorylation of UPF3B contributes to the ER stress-induced pathogenesis. In conclusion, our data demonstrated that UPF3B plays a critical role in ER homeostasis by inhibiting the UPR and preventing cell apoptosis due to ER stress.

Results

NMD regulates the UPR signaling pathway

NMD is the translation-coupled mRNA degradation pathway that functionally eliminates the overproduction of truncated proteins both in the ER and in the cytosol. To test whether inhibition of NMD affects ER stress, three protein synthesis inhibitors with different mechanisms of translation inhibition were selected for treatment of HEK293T cells. Puromycin, an aminoacyl-tRNA analogue, causes premature termination of translation and leads to rapid polysome degradation. Cycloheximide binds to 80S ribosomes and prevents translocation of tRNA during translation. Both translational and NMD inhibitors led to the activation of phosphorylation of eIF2α, PERK and IRE1α and increased protein levels of XBP1s, ATF6 and CHOP. However, Harringtonine, which only blocks translational elongation without inhibiting NMD [25], neither caused the increase in eIF2α phosphorylation nor led to ER stress (Fig. 1A).

Next, three key factors, UPF1, UPF2 and UPF3B, were each depleted in HEK293T cells. In all UPF-depleted cells, phosphorylation of PERK and eIF2α and protein levels of ATF6, XBP1s, BiP and CHOP were apparently upregulated (Figs. 1B and 1C), similar to treatment with puromycin or cycloheximide. These data suggest that the maintenance of proper NMD function is critical for balancing the basal activation

of the UPR pathway and consequently suppressing over-activation of ER stress. We then investigated the effect of NMD on apoptosis. In all three UPF-depleted cell lines, cell apoptosis was apparently increased (Figs. 1D and 1E). To address whether the inhibition of NMD-induced apoptosis was mediated by the activation of ER stress, the IRE1α inhibitor Kira6 was selected to treat the UPF-depleted cells. Kira6 is an imidazopyrazine-based small molecule that competitively binds the ATP-binding site of the kinase domain of IRE1α and blocks the kinase and RNase activities of IRE1α [26, 27]. Cell apoptosis induced by NMD disruption is significantly alleviated by Kira6 treatment. This suggests that the high level of cell apoptosis upon NMD disruption is mediated by activation of ER stress, possibly through a branch of the IRE1α pathway.

Unique regulation role of UPF3B in IRE1α signaling pathway

Surprisingly, UPF3B has a distinct role in IRE1α phosphorylation compared to UPF1 and UPF2. In shUPF3B cells, IRE1α phosphorylation was apparently increased, but this was not the case in shUPF1 and shUPF2 cells. Instead, IRE1α phosphorylation was slightly further inhibited in shUPF2 cells (Fig. 2A). Knockdown of UPF1 or UPF2 slightly increased the protein level of UPF3B, but depletion of UPF3B had no effect on the levels of UPF1 and UPF2. Instead, the levels of IRE1α phosphorylation and XBP1s were strongly reduced in cells overexpressing UPF3B. In addition to two ER stress markers, the expression levels of two downstream effectors, BiP and CHOP, were also significantly lower than in normal cells (Fig. 2B).

Since UPF3B knockdown leads to apoptosis, the effects of UPF3B on apoptosis during ER stress were investigated. The ER stress inducer thapsigargin (Tg) was chosen to treat the cells. Tg is a sesquiterpene lactone that is permeable to cells and induces ER stress by specifically inhibiting the Ca^{2+}-ATPase within the ER [28]. The results showed that knockdown of UPF3B enhanced apoptosis induced by Tg treatment, but overexpression of UPF3B inhibited Tg-induced apoptosis (Fig. 2C-2E). This suggests that UPF3B is involved in the regulation of apoptosis induced by ER stress.

UPF3B uniquely affected the phosphorylation of IRE1α, rather than UPF1 and UPF2. It is interesting to explore the underlying mechanism by which UPF3B inhibits IRE1α phosphorylation. First, the endogenous interaction between IRE1α and UPF3B was confirmed by co-immunoprecipitation assays in both HEK293T cells and U2OS osteosarcoma cell lines (Figs. 2F and 2G). To exclude that the interaction between IRE1α and UPF3B is mediated by RNAs, since both are RNA binding proteins, cell lysates were pretreated with RNase A and IRE1α still immunoprecipitated UPF3B (Figure S1). This suggests that the interaction occurs in an RNA-independent manner. Immunofluorescence experiments and colocalization analysis demonstrated that UPF3B as a shuttle protein, partially colocalized with IRE1α at ER loci (Fig. 2H and S2). Taken together, these data suggest that UPF3B directly interacts with IRE1α at the ER and modulates the activation of the IRE1α-XBP1s branch.

UPF3B inhibits the phosphorylation of IRE1α by binding to its kinase domain

IRE1α is a transmembrane protein consisting of a sensory domain in the ER lumen, the transmembrane segments and two cytoplasmic side domains including the regulated kinase domain and the RNase domain [29, 30]. UPF3B contains a conserved RNA recognition motif (RRM)-like domain that mediates interaction with the MIF4G (middle portion of eIF4G) domain of UPF2, a middle domain, and an EJC binding motif (EBM) [31]. To investigate the structural requirements for IRE1α interaction with UPF3B, different domain deletions or truncation mutants for IRE1α (Fig. 3A) and UPF3B (Fig. 3B) were generate to analyze their interaction regions by co-immunoprecipitation assays and GST pulldown experiments. Among these IRE1α mutants, IRE1α$^{\Delta KR}$, in which the kinase and RNase domains were deleted, did not interact with UPF3B. However, IRE1α$^{\Delta R}$ with the RNase domain deleted, IRE1α^{KR} containing the kinase and RNase domains, and IRE1α^{K} containing only the kinase domain interacted with UPF3B (Figs. 3C and 3D). This suggests that the kinase domain of IRE1α is the UPF3B binding site. In the UPF3B mutants, removal of the RRM-like domain abolished the interaction between UPF3B and IRE1α (Figs. 3E and 3F), suggesting that the RRM-like domain of UPF3B is the key motif for IRE1α and UPF3B interaction. This was further confirmed by two-way immunoprecipitation analysis between UPF3B^{RRM} and IRE1α^{K} in HEK293T cells (Fig. 3G). However, overexpression of UPF3B^{RRM} alone only minimally suppressed IRE1α phosphorylation, in contrast to overexpression of UPF3B^{WT} (Figure S3), suggesting that the full length of UPF3B is required for the modulation of IRE1α phosphorylation.

UPF3B prefers to bind unphosphorylated IRE1α

Tg and another ER stress inducer, tunicamycin (Tm), were chosen to treat the cells to investigate whether the interaction between IRE1α and UPF3B was affected under ER stress activation. Tm is a natural nucleoside antibiotic that induces ER stress by inhibiting the protein glycosylation pathway [32]. When cells were treated with Tm (10 μg/mL) or Tg (2 μM) for 1 and 3 h, respectively, the phosphorylation level of IRE1α was significantly upregulated, but the expression level of UPF3B was not affected (Fig. 4A). However, interaction between IRE1α and UPF3B was significantly decreased in the cells treated with either Tm or Tg, and the strength of the interaction was negatively correlated with the phosphorylation level of IRE1α (Fig. 4B and S4). To investigate further whether the interaction was mainly between unphosphorylated IRE1α and UPF3B, two IRE1α inhibitors, STF-083010 and Kira6, were selected to test the interaction. Unlike Kira6, which inhibited the phosphorylation and kinase activity of IRE1α, STF-083010 forms a selective Schiff's base with a catalytic lysine in the RNase active site of IRE1α and is a specific inhibitor of IRE1α endonuclease activity rather than kinase activity [33]. Indeed, neither the phosphorylation of IRE1α nor the interaction between IRE1α and UPF3B appeared to be affected in STF-083010 treated cells, although the splicing form of XBP1 was slightly inhibited (Fig. 4C). In contrast, Kira6 treatment abolished the phosphorylation of IRE1α and the splicing of XBP1, and the interaction between IRE1α and UPF3B was strongly enhanced (Fig. 4C). This suggests that UPF3B preferentially binds to the kinase domain of IRE1α in the non-phosphorylation state.

The IRE1α^{D123P} mutation, which abolishes IRE1α dimerization and activation [34], and the IRE1α^{K599A} mutation in the ATP-binding pocket of the kinase domain [35] have been confirmed to inhibit the IRE1α

phosphorylation. In contrast, the IRE1α^{K907A} mutant was RNase-defective but caused high phosphorylation of IRE1α [36]. These three functional mutants were used in comparison with IRE1α wild-type to further investigate the interaction between IRE1α and UPF3B (Fig. 4D). Consistent with previous studies, phosphorylation of IRE1α was strongly inhibited in the IRE1α^{D123P} and IRE1α^{K599A} mutants, but enhanced in the IRE1α^{K907A} mutant. More importantly, the interaction was apparently stronger between UPF3B and IRE1α^{D123P} or IRE1α^{K599A}, but weaker between UPF3B and IRE1α^{K599A} compared to the wild-type interaction (Fig. 4D). This further confirmed that phosphorylation of IRE1α abolishes the interaction with UPF3B. Since phosphorylation at Ser724 of IRE1α is the predominant activated form of the kinase, we substituted Ser724 of IRE1α with aspartic acid (designated IRE1α^{S724D}) or alanine (IRE1α^{S724A}) to mimic the retention or loss of its kinase activity, respectively. UPF3B has a much stronger interaction with IRE1α^{S724A}, but a much weaker interaction with IRE1α^{S724D} compared with IRE1α^{WT} (Fig. 4E). In conclusion, the strength of the interaction between IRE1α and UPF3B was negatively correlated with the phosphorylation level of IRE1α (Figure S4). Next, a bimolecular fluorescence complementation (BiFC) assay was conducted to confirm the interaction. IRE1α-Vn173, IRE1α^{S724A}-Vn173 and IRE1α^{S724D}-Vn173 were co-transfected with UPF3B-Vn155 in U2OS cells, respectively. The results showed that the interaction was mainly in the cytoplasm, and the interaction was stronger in IRE1α^{S724A}-Vn173 and UPF3B-Vn155 than IRE1α^{S724D}-Vn173 (Fig. 4F), confirming the critical role of phosphorylation at Ser724 of IRE1α in the interaction between IRE1α and UPF3B.

BiP and UPF3B jointly control the activation of IRE1α

IRE1α contains four domains, including a sensory domain in the ER lumen, transmembrane segments and two domains in the cytoplasmic side: the regulated kinase domain and the RNase domain (Fig. 5A). BiP has been reported to interact with the sensory domain of IRE1α to attenuate its activation [37]. Under Tm or Tg transient treatment for 1 h, BiP was suppressed, the phosphorylation of IRE1α was enhanced and accordingly, the interaction between BiP and IRE1α was attenuated (Fig. 5B). Restoration of BiP decreased IRE1α phosphorylation and enhanced the interaction between IRE1α and UPF3B (Fig. 5C). In si-BiP cells, the phosphorylation level of IRE1α was increased and the interaction between UPF3B and IRE1α was inhibited (Fig. 5D). These results suggest that BiP in the ER lumen affects the interaction of IRE1α and UPF3B in the cytoplasmic side possibly via modulation of IRE1α activation.

Overexpression of UPF3B downregulated the levels of phosphorylated IRE1α and BiP, and consequently reduced the interaction between IRE1α and BiP (Fig. 5E). This implies that UPF3B potentially affects the balance of ER stress by limiting the activation of IRE1α and the expression of BiP. During ER stress activation, the protein level of IRE1α was not affected in UPF3B-overexpressing cells, but the extent of IRE1α phosphorylation and the level of XBP1s were also much less increased compared to the normal cells (Figs. 2B, 5F-5G). The interactions between IRE1α and BiP were strongly suppressed due to the downregulation of BiP levels. This may be because UPF3B negates the phosphorylation of IRE1α via protein interactions in UPR and consequently suppresses the expression of BiP. In shUPF3B cells, phosphorylation of IRE1α was still inhibited by overexpression of BiP (Figure S5A), but the efficiency of

inhibition was only achieved at higher levels of BiP expression than that in normal cells (Figure S5B). When siBiP was used in UPF3B knockdown cell lines, phosphorylated IRE1α was not further upregulated (Figure S5C). The results showed that UPF3B may have a concerted regulatory role in IRE1α phosphorylation together with BiP, but is not fully dependent on BiP expression. In the BiP knockdown cell lines, overexpression of UPF3B inhibited IRE1α phosphorylation (Figure S5D), indicating that the functions of UPF3B and BiP are independent and redundant in regulating the activity of IRE1α.

UPF2 contains three conserved MIF4G (middle part of eIF4G) structural domains [38, 39]. UPF2 interacts with UPF3B through its third MIF4G structural domain (Fig. 5H) and with UPF1 through its C-terminus, forming the central component of the ternary UPF complex. When the UPF2 MIF4G-3 segment was overexpressed in cells (Fig. 5I), the interaction of UPF3B with IRE1α was apparently inhibited and the phosphorylation of IRE1α was increased. Furthermore, overexpression of UPF3B not only decreased the phosphorylation of IRE1α but also precipitated more UPF2 and IRE1α in a dose-dependent manner (Fig. 5J). Two UPF3B mutants [31], $UPF3B^{K52E}$ or $UPF3B^{R56E}$, which disrupt the interaction of UPF2 with UPF3B, were applied to test the interaction between UPF3B and UPF2 or IRE1α. Either $UPF3B^{K52E}$ or $UPF3B^{R56E}$ enhanced the interaction between UPF3B and IRE1α, whereas the EJC binding domain deletion mutant had no such effect (Figure S6). Nevertheless, these mutants inhibited IRE1α phosphorylation compared to the control, suggesting that free UPF3B, rather than the intact NMD complex, plays an important role in suppressing IRE1α activation.

UPF3B attenuates IRE1α dimerization and oligomerization under ER stress

During ER stress, activated IRE1α forms higher order oligomers or clusters in stressed cells [40]. Since UPF3B negates IRE1α activation in cells by direct interaction, it is interesting to confirm whether UPF3B restricts the oligomerization of IRE1α during ER stress. IRE1α-GFP was transfected into the control and the shUPF3B cells as an oligomerization indicator. Fluorescent aggregation of IRE1α-GFP was evident under both Tm and Tg treatment for 1 and 3 h, respectively (Fig. 6A), and was further enhanced in shUPF3B cells (Figs. 6B and 6C). Statistical analysis showed that a higher proportion, larger area and higher fluorescence intensity of aggregated clusters appeared in the shUPF3B cells compared to control cells (Figs. 6D and 6F). This suggests that UPF3B is required to negate the aggregation of IRE1α under ER stress. Activation of IRE1α depends on autophosphorylation induced by homodimerization. To address whether UPF3B affects IRE1α dimerization, two different tagged IRE1α, IRE1α-Flag and IRE1α-HA, were co-expressed in cells. The dimerization of IRE1α was strongly inhibited with the dosage correlating with the overexpression of UPF3B (Fig. 6G).

The phosphorylation and genetic mutation of UPF3B abolishes the interaction with IRE1α

A single nucleotide substitution, 478T > G, has been identified in exon 5 of the non-syndromic X-linked mental retardation (XLMR) family [24]. This nucleotide change caused the conversion of the 160th tyrosine

to aspartic acid (Y160D). The tyrosine residue at this site is conserved in UPF3B in plants and animals, implying its physiological importance for UPF3B function. However, the underlying pathogenesis remains unknown. We overexpressed two UPF3B mutants, UPF3B^{Y160F} and UPF3B^{Y160D} and immunoprecipitated endogenous IRE1α to detect the interactions between IRE1α and both mutants. UPF3B^{Y160D} showed a weaker interaction with IRE1α compared to UPF3B^{WT} and UPF3B^{Y160F} (Fig. 7A), suggesting that UPF3B^{Y160D} losses the function to inhibit IRE1α activation in suppressing ER stress. The oligomerization of IRE1α was examined by complementation of UPF3B^{WT}, UPF3B^{Y160F} or UPF3B^{Y160D} in shUPF3B cell lines under ER stress (Figure S7). Statistical analysis showed that in shUPF3B cells, the proportion, area and fluorescence intensity of aggregated IRE1α clusters were not suppressed by UPF3B^{Y160D} overexpression which was similar to control cells, but were apparently suppressed by complementation of UPF3B^{WT} and UPF3B^{Y160F} under ER stress. Taken together, these data suggest that Y160D mutation may result in chronic high levels of ER stress, which may lead to some neurodevelopmental disorders.

Given that UPF3B^{Y160D} disrupts the interaction between UPF3B and IRE1α, which is similar to the conditions of ER stress activation, we hypothesized that not only IRE1α but also UPF3B is regulated by phosphorylation modifications in stress stimuli. First, we examined the changes in serine-threonine phosphorylation of UPF3B in response to ER stress induced by Tm or Tg for 3 h (Fig. 7B). The phosphorylation of UPF3B was increased in a time-dependent manner after 1, 3 or 6 h of Tg treatment, similar to the IRE1α phosphorylation (Fig. 7C). The results showed that the phosphorylation of UPF3B were enhanced in response to ER stress. To determine the site where UPF3B was phosphorylated, phosphorylation mapping mass spectrometry was applied to precipitated UPF3B from HEK293T cells (Fig. 7D). Among the six phosphorylation sites identified, T169, T197 or T198 phosphorylation sites were present in the RRM domain that interacts with IRE1α. To address the key phosphorylation sites, we made three pair mutants, UPF3B^{T169A} and UPF3B^{T169D}, UPF3B^{T197A} and UPF3B^{T197D}, and UPF3B^{T198A} and UPF3B^{T198D}, mimicking the unphosphorylated or phosphorylated status of UPF3B. The results showed that only UPF3B^{T169D} significantly inhibited the interaction between IRE1α and UPF3B, which is similar to the genetic mutation of UPF3B^{Y160D}, while the mutations at the other two sites did not significantly alter the interaction (Figs. 7E-7G). In conclusion, the strength of the interaction between IRE1α and UPF3B was not only negatively correlated with the phosphorylation level of IRE1α, but also affected by the phosphorylation of UPF3B (Figure S8).

The interaction of UPF3B^{Y160D} with UPF2 was also inhibited compared to UPF3B^{WT} and UPF3B^{Y160F} (Fig. 7H). Therefore, the UPF3B^{Y160D} mutant impaired the interaction of UPF3B with both IRE1α and UPF2. This raises the question whether XLMR parthenogenesis is due to the loss of the ability of UPF3B^{Y160D} to suppress ER stress or maintain NMD efficiency, or both. We therefore examined whether the potential phosphorylation site of UPF3B would affect its interaction with UPF2. UPF3B^{T169D} also appeared to inhibit the interaction with UPF2 compared to UPF3B^{WT}, UPF3B^{T197D} and UPF3B^{T198D} (Figs. 7H-7J). Also, the two mutations UPF3B^{Y160D} and UPF3B^{T169D}, which are suppressed in the interaction with IRE1α, also attenuate the inhibition of apoptosis compared with the restoration of

UPF3B^{WT}, UPF3B^{Y160F} or UPF3B^{T169A}, respectively, in shUPF3B cell lines under physiological conditions and during ER stress (Figs. 7K-7N).

The dual role of UPF3B in NMD and ER stress

Our study provides insights into the direct linkage via UPF3B interactions between two quality control pathways at the ER locus. Under physiological conditions, the monomeric IRE1α kinase endonuclease remains in an inactive form by binding to BiP at the sensory domain and UPF3B at the kinase domain on both sides of the ER lumen and cytoplasm. Upon ER stress, unfolded proteins compete with IRE1α for BiP, and stress-induced phosphorylation of UPF3B losses its ability to suppress IRE1α activation, allowing IRE1α to dimerize, activate its kinase activity and mediate its autophosphorylation, leading to regulated IRE1α-dependent decay. The dimerized IRE1α is further oligomerized, and forms foci that correlate with the activation of IRE1α-catalyzed splicing endonuclease activity. In conclusion, UPF3B plays an important role in negating UPR activation by suppressing the high-order oligomerization of IRE1α required for its activation by autophosphorylation. UPF3B is phosphorylated during ER stress, UPF3B^{T169} phosphorylation and the UPF3B^{Y160D} genetic mutation fail to interact with IRE1α and UPF2 and are unable to antagonize ER stress-induced apoptosis compared to UPF3B^{WT}, which may be related to the pathogenesis in XLMR or other neuronal degenerative diseases. Overall, our data demonstrate that UPF3B plays a critical role in ER homeostasis by inhibiting the UPR and preventing ER stress-induced cell apoptosis.

Discussion

The UPR restores ER protein homeostasis of by reducing ER stress and damage to a physiological level. It promotes protein folding by dealing with proteins already accumulated in the ER, such as upregulating the expression of molecular chaperones (e.g. BiP) or folding-related enzymes, and activating the ER-related protein degradation system to deal with those proteins that do not fold properly under stress conditions. It also modulates the balance of translation and prevents further protein accumulation in the ER [41]. ER stress, in which the UPR is over-activated, results in structural and functional disturbances of the ER, accompanied by the accumulation of misfolded proteins and changes in calcium homeostasis [42]. Overactivation of the UPR alters ER stress sensors and effector proteins, including phosphorylation levels of PERK and IRE1α, and protein levels of XBP1s, ATF6 and downstream factors such as phosphorylated eIF2α, BiP and CHOP, which are hallmarks of ER stress activation. Consequently, these changes lead to attenuated translation, induction of molecular chaperone protein synthesis in the ER, and accelerated degradation of misfolded proteins. When ER stress signaling exceeds the self-regulatory capacity of the cell, it activates apoptosis-related signals and induces cell apoptosis. Therefore, the level of ER stress determines the fate of the cell, either adapting to the changes or leading to cell death. Studies have shown that the occurrence and development of many diseases of the human nervous system, such as Parkinson's and Alzheimer's diseases [43, 44], are related to ER stress.

NMD is a conserved post-transcriptional quality control mechanism in eukaryotes that plays an important role in various physiological and pathological processes such as neurogenesis, synapse formation, nervous system development and disease [45]. Most NMD studies have focused mainly on the cytosolic mechanism for controlling gene expression. Few studies have addressed the physiological function of NMD at ER loci but translation also occurs at the ER. The specific biological functions of NMD in ER stress modulation beyond gene expression control remain unclear. Understanding whether ER stress is physiologically affected by NMD is important to our knowledge of the intercellular linkage between different quality control pathways. In our study, depletion of any of the UPF proteins activates ER stress and increases cell apoptosis. When UPF1, UPF2 or UPF3B were depleted in HEK293T cells, phosphorylation of PERK and eIF2α, and protein levels of ATF6, BiP and CHOP were increased, suggesting that proper levels of NMD factors maintain the suppressive role in ER stress or UPR signaling pathways. Thus, efficient NMD may be important to prevent inappropriate and prolonged activation of the UPR. Cell apoptosis induced by NMD disruption is significantly alleviated by inhibition of ER stress, suggesting that apoptosis induced by NMD disruption is probably mediated by ER stress activation and implicating an underlying link between them in disease pathogenesis.

Among the three branches of ER stress, the IRE1α/XBP1 axis is the most conserved pathway. IRE1 is a type I ER transmembrane glycoprotein with Ser/Thr receptor protein kinase activity and specific endonuclease activity [46]. IRE1α is activated to undergo dimerization and autophosphorylation, thereby activating the cytoplasmic endonuclease domain. Consequently, the downstream XBP1 mRNA is alternatively spliced and translated into the short protein isoform, XBP1s [47]. XBP1s binds to ER-related cis-transcription elements and upregulates the expression of ER stress-related proteins such as BiP to promote ER membrane biogenesis and improve the protein folding capacity of the ER to negate further stress [48]. Research has shown that scaffold protein receptor for activated C-kinase 1 (RACK1) interacts with IRE1α in pancreatic β cells and primary islets in response to glucose stimulation or ER stress [49]. The ER luminal chaperone ERdj4/DNAJB9 represses IRE1 activation by promoting the complex between BiP and IRE1α at the ER lumen [50]. Li *et al*. found that IRE1α forms a complex with Sec61/Sec63 translocons in cells. Sec63 mediates BiP binding to IRE1α, thereby inhibiting IRE1α oligomerization and attenuating IRE1α signaling during prolonged ER stress [51]. Knockdown of ribosome-associated complex (RAC) has been shown to sensitize mammalian cells to ER stress and selectively interfere with IRE1 branch activation [52]. Higher order oligomerization of the IRE1α kinase/endonuclease is dependent on RAC.

In the study, IRE1α phosphorylation was specifically enhanced UPF3B knockdown and suppressed by UPF3B overexpression, but not by UPF1 and UPF2. This suggests that in addition to its role in NMD, UPF3B is specifically involved in the IRE1α/XBP1 axis of the UPR. Overexpression of UPF3B inhibited IRE1α-induced ER stress and cell apoptosis, implying a reciprocal role between IRE1α and UPF3B at ER loci in cell fate determination. Indeed, we confirmed that UPF3B directly interacts with IRE1α by GST pull-down and IP assays, and partially colocalizes with IRE1α by immunofluorescence and BiFC. The tight regulatory interplay between these two proteins was addressed in this study. The kinase domain of IRE1α interacts with the RRM-like domain of UPF3B. Under stress conditions, the UPF3B-IRE1α interaction was

apparently abolished, mainly due to high phosphorylation of IRE1α. The phosphorylation level of IRE1α is controlled by the phosphorylation of serine at position 724 [53]. The phosphorylation-loss mutant IRE1α^{S724A} and IRE1α^{WT} have a higher binding capacity to UPF3B than the phosphorylation mutant IRE1α^{S724D}. This confirms that UPF3B has a stronger interaction with non-phosphorylated IRE1α than with phosphorylated IRE1α, suggesting that UPF3B may be involved in the suppression of IRE1α phosphorylation. Further analysis of functionally relevant point mutations such as the oligomerization-defective mutation IRE1α^{D123P}, the kinase activity-defective mutation IRE1α^{K599A}, the RNase activity-defective mutation IRE1α^{K907A} and inhibitors of kinase and RNase activity, supported that UPF3B inhibits IRE1α activation through its direct interaction with latent IRE1α.

The UPR signaling cascade is maintained at a basal level by BiP, a major ER molecular chaperone that represses three signaling transducers through luminal interactions. In cells overexpressing BiP, the phosphorylation of IRE1α was inhibited and the interaction between IRE1α and UPF3B was correspondingly enhanced. BiP depletion increased the phosphorylation of IRE1α and decreased the interaction between IRE1α and UPF3B. Both suggest that the level of BiP affects the interaction between IRE1α and UPF3B. Interestingly, overexpression of UPF3B not only attenuated ER stress, but also reduced BiP levels. Furthermore, in shUPF3B cells, more BiP expression was required to return IRE1α phosphorylation to baseline, suggesting that UPF3B functions cooperatively and redundantly in suppressing IRE1α activation at the cytoplasmic side. All this confirms that the interaction between BiP and IRE1α in the luminal side potentially mutually interplays with the interaction between UPF3B and IRE1α in the cytoplasmic side.

Phosphorylated IRE1α is prone to dimerization and further oligomerization, which depends on the activation of its cytoplasmic kinase domain. In addition to biochemical evidence of oligomerization, live cell microscopy of IRE1α using fluorescent protein labeling shows that its accumulation in the ER membranes is the hallmark of the extent of ER stress [54]. Using the same strategy, we demonstrated that UPF3B knockdown affected IRE1α clustering. IP assay proved that the oligomerization of IRE1α was apparently inhibited by UPF3B. These results further confirmed that UPF3B suppresses ER stress by inhibiting IRE1α phosphorylation and clustering under stress, such as exposure to Tg and Tm.

UPF3B missense mutations are found in patients with schizophrenia and X-linked intellectual disability (XLID). Expression of these UPF3B mutants in neural stem cells impairs neuronal differentiation and reduces axonal branching [55]. Chronic activation of ER stress also leads to the formation and accumulation of protein aggregates, partly associated with disruption of synaptic function and, in some cases, with neuronal death [56]. Neuronal cells are particularly sensitive to protein misfolding and ER dysfunction has been implicated in many neurodegenerative diseases [57]. The tyrosine residue UPF3B^{Y160} is highly conserved in vertebrates, *Drosophila melanogaster*, and *Caenorhabditis elegans*. The UPF3B^{Y160D} mutation is genetically linked to XLID. UPF3B^{Y160D} significantly inhibits both the interactions of UPF3B with IRE1α and UPF2, suggesting that the missense mutation of UPF3B losses its suppressive function in IRE1α activation, potentially leading in chronic UPR activation for the development of some

neurodegenerative diseases. However, the relevance of this effect to the mental retardation caused by this genetic mutation remains to be investigated in animal models. Similar to the UPF3B^{Y160D} mutant, the phosphorylation of UPF3B was apparently upregulated under ER stress conditions, and the phosphorylation of Thr169 of UPF3B attenuated both the UPF3B-IRE1α interaction and the UPF2-UPF3B interaction. In contrast to UPF3B^{WT}, UPF3B^{Y160F} and UPF3B^{T169A}, restoration of various UPF3B mutants including UPF3B^{Y160D} and UPF3B^{T169D} in shUPF3B cells, failed to suppress cell apoptosis either in both normal and stress conditions, further supporting that these two interactions paly the important role in ER stress-related pathogenesis.

Activation of the UPR signaling pathways reduces overall protein synthesis, increases ER protein folding capacity, and promotes degradation of misfolded proteins [58]. If the UPR fails to achieve ER homeostasis in a timely manner, programmed cell death would be triggered as a cellular response. We discovered the novel function of UPF3B in antagonizing ER stress by specifically inhibiting IRE1α activation under physiological conditions. UPF3B inhibits the formation of higher order oligomers of IRE1α but not in phosphorylated UPF3B during ER stress. UPF3B^{T169D} and UPF3B^{Y160D}, inhibit its interaction with IRE1α and UPF2, and cause the apparent cell apoptosis, providing a potential target for therapeutics to ameliorate the deleterious outcome of ER stress. For the first time, our study provides the evidence for the interplay role of UPF3B in NMD and ER stress and a new perspective on the physiological significance of NMD in modulating ER stress.

Materials and methods

Cell culture and transfection

HEK293T (ATCC, CRL-3216) and U2OS (ATCC, HTB-96) cell lines were preserved in our laboratory. All the cell lines were regularly tested and ensured to be negative for mycoplasma contamination. The cells were cultured in Dulbecco's modified Eagle's medium (DMEM, Thermo Fisher, USA) containing 10% fetal calf serum (BI, German) at 37°C in a CO_2 incubator (Thermo Fisher, USA), 0.25% trypsin-EDTA, and puromycin that were obtained from Invitrogen (Carlsbad, CA, USA). Lipofectamine 2000 and 3000 were obtained from Invitrogen (Carlsbad, CA, USA). According to the Lipofectamine 3000 operating instructions, plasmids, P3000 and Lipofectamine 3000 were added into the serum-free Opti-MEM and left for 5 min. Stand for 15 min after mixing, cells were added to transfection medium and cultured at 37℃ for 5 h and then replaced the complete medium.

Chemical reagents

Thapsigargin (Tg) and tunicamycin (Tm) were purchased from Beyotime Biotech (Shanghai, China). STF-083010 and Kira6 were purchased from Selleck (Shanghai, China). Hoechst 33342 and 4',6-diamidino-2-phenylindole (DAPI) were obtained from Beyotime Biotech (Shanghai, China).

Antibodies

The antibodies applied in this study are listed in Supplementary Table 1.

Plasmids

The human IRE1α plasmid was purchased from Addgene (#13009), and the human UPF3B plasmid was purchased from Sino Biological (HG16941-CF). The expression plasmids for the deletion mutants and point mutations of IRE1α and UPF3B were cloned into pcDNA4 with the Flag tag in-frame at the N terminus. Flag, Myc, and HA epitope tags were added to the C-terminal coding ends of the IRE1α and UPF3B constructs. For BiFC analysis, VN173 and VC155, which are complementary fragments of Venus, were fused to the C-terminal of IRE1α and the N-terminal of UPF3B, respectively. All constructs were verified by DNA sequencing.

Western blot

The total cell lysates were prepared by using cold radioimmunoprecipitation assay (RIPA) lysis buffer (50 mM Tris-HCl, 150 mM NaCl, 1% Triton X-100, pH 7.8) containing protease and phosphatase inhibitors on ice for 30 min, and then centrifuged the mixture for 10 min at 14 000×g. The lysates were subjected to sodium dodecyl sulfate–polyacrylamide gel electrophoresis (SDS-PAGE) and transferred to polyvinylidene fluoride membranes (Millipore, USA). We used an enhanced chemiluminescence (ECL) mix to visualize the proteins.

shRNA-mediated gene knockdown

RNA interference was carried out by using a shRNA expressing H1 retroviral system. The RNA-mediated interference of UPF1, UPF2 and UPF3B was performed in HEK293T cells using pLKO.1 vector encoding the shRNA sequence. UPF1: 5′- CCTGCGTGGTTTACTGTAATA – 3′, UPF2: 5′- CATCAGAGTCAGTGCTATAAA – 3′, UPF3B: 5′- GAAGCCTTGTTCCGATCTAAT – 3′, BiP: 5′- GCTCGACTCGAATTCCAAAGA – 3′, respectively. The knockdown efficiency of the target genes was validated by western blotting.

Transfection of small inhibitory RNA

Cells were cultured to 70–80% confluence in 10% FBS supplemented DMEM and transfected with siRNA using Lipofectamine 3000 reagent according to the manual instruction. A non-targeting 20–25 nucleotide sequence siRNA was used as a negative control. The list of primers used for siRNA is as follows: siNC-sense: 5′-UUCUCCGAACGUGUCACGUTT – 3′, siBiP-sense: 5′- CCUUCGAUGUGUCUCUUCUTT – 3′.

Flow cytometry assay

The cell apoptosis was detected with an Annexin-V-FITC/PI detection kit purchased from Beyotime Biotechnology (Shanghai, China). Cells were precipitated by centrifugation at 1 000g for 5 min, and discard the supernatant. The collected cells were washed twice with cool PBS, precipitated by centrifugation and gently resuspended by adding 500 μL Annexin V buffer. 5 μL Annexin V-FITC and 5 μL propidium iodide staining solution were added and gently mixed. Incubate for 15 min at room temperature (20–25°C) in the dark. Then the cells were immediately detected with the flow cytometer (FACSCalibur, BD, USA).

Immunofluorescence

U2OS and HEK293T cells were cultured on cell slides inside a 24-well plate for 24 h. The medium was then decanted, and the wells were washed three times with cold PBS. The cells were then fixed in 4% paraformaldehyde for 15 min and permeabilized in 0.5% Triton X-100 for 5 min. After washing three times with PBS, the cells were blocked for 1 h in PBS with 5% bovine serum albumin. The primary antibodies were diluted by 1:100 in PBS with 1% bovine serum albumin and incubated 1 h. After washing three times with PBS, Alexa Fluor 488 anti-rabbit and Alexa Fluor 594 anti-mouse antibodies (Cell Signal Technology, USA) were added to the antibody dilution buffer at 1:500 dilutions. We then added DAPI to the slides and incubated for 2 min at room temperature. After washing the slides three times with PBS, we mounted them using an antifade reagent (Invitrogen, USA). We acquired images using a two-photon super-resolution point scanning confocal microscope (AX, Nikon, Japan) and selected representative images for each sample.

Co-immunoprecipitation

U2OS and HEK293T cells were seeded in 60 mm culture dishes and transfected using Lipofectamine 2000 reagent (Invitrogen, USA). After transfection for 24 h, we lysed the cells in NETN buffer (20 mM Tris-HCl pH 8.0, 100 mM NaCl, 1 mM EDTA, 0.5% NP-40) with 1% protease and phosphatase inhibitor cocktail (Sigma Aldrich, USA). The cell extract was used to immunoprecipitated Flag with anti-Flag (M2) magnetic beads as described, and the beads were then washed three times with NETN buffer. We analyzed the samples by western blotting with antibodies.

BiFC analysis

We grew U2OS cells on coverslips inside a 24-well plate at 37°C in a cell culture incubator. The UPF3B-VC155 and IRE1α-VN173 constructs and the mutants were transfected with Lipofectamine 2000 according to the manufacturer's instructions. After transfection for 24 h, the nuclear DNA of the living cells was stained with Hoechst 33342. We acquired images using a two-photon super-resolution point scanning confocal microscope (AX, Nikon, Japan) and selected representative images for each sample. 40–50 cells from three independent biological experiments were randomly selected for statistical analysis.

Statistical analysis and reproducibility

Quantitative data are expressed as the mean ± standard error of the mean (SEM) of at least three independent experiments. Statistical differences between multiple comparisons were analyzed by one-way or two-way analysis of variance (ANOVA) with Bonferroni correction where appropriate. A two-tailed unpaired t-test was used to compare the means of the two groups. All western blots and fluorescence tests were performed on at least three independent biological experiments to ensure reproducibility, and representative images were shown.

Declarations

Acknowledgements

We acknowledge supports from the Joint Fund of National Natural Science Foundation of China and Guangdong Province (U1901207), Laboratory of Lingnan Modern Agriculture Project (NZ2021016), the National Natural Science Foundation of China (32102718), Guangdong Basic and Applied Basic Research Foundation (2022B1515130003, 2023A1515011044).

We would like to thank Dr. Xiao Huang and Prof. Yu Sun for language editing and proofreading.

Author contributions

XS carried out most experiments, XQ, TJ, XL, and ZW contributed to several experiments, XS, RL, JW and YD conceived the study, RL, JW and YD helped with data analyses and discussions. JJ, PM and QC help with several experimental design, and XS and JW wrote the manuscript.

Conflict of interest

The authors declare that they have no conflict of interest.

References

1. Benhamron S, Hadar R, Iwawaky T, So JS, Lee AH, Tirosh B. Regulated IRE1-dependent decay participates in curtailing immunoglobulin secretion from plasma cells. *European journal of immunology* 2014, **44**(3)**:** 867-876.
2. Cnop M, Foufelle F, Velloso LA. Endoplasmic reticulum stress, obesity and diabetes. *Trends in molecular medicine* 2012, **18**(1)**:** 59-68.
3. Hwang J, Qi L. Quality Control in the Endoplasmic Reticulum: Crosstalk between ERAD and UPR pathways. *Trends in biochemical sciences* 2018, **43**(8)**:** 593-605.
4. Read A, Schröder M. The Unfolded Protein Response: An Overview. *Biology* 2021, **10**(5).
5. Hotokezaka Y, Katayama I, Nakamura T. ATM-associated signalling triggers the unfolded protein response and cell death in response to stress. *Communications biology* 2020, **3**(1)**:** 378.
6. Pinkaew D, Chattopadhyay A, King MD, Chunhacha P, Liu Z, Stevenson HL*, et al.* Fortilin binds IRE1α and prevents ER stress from signaling apoptotic cell death. *Nature communications* 2017, **8**(1)**:** 18.
7. Liu Z, Lv Y, Zhao N, Guan G, Wang J. Protein kinase R-like ER kinase and its role in endoplasmic reticulum stress-decided cell fate. *Cell death & disease* 2015, **6**(7)**:** e1822.
8. Hetz C, Zhang K, Kaufman RJ. Mechanisms, regulation and functions of the unfolded protein response. *Nature reviews Molecular cell biology* 2020, **21**(8)**:** 421-438.
9. Mitra S, Ryoo HD. The unfolded protein response in metazoan development. *Journal of cell science* 2019, **132**(5).

10. Lopata A, Kniss A, Löhr F, Rogov VV, Dötsch V. Ubiquitination in the ERAD Process. *International journal of molecular sciences* 2020, **21**(15).
11. Park KW, Eun Kim G, Morales R, Moda F, Moreno-Gonzalez I, Concha-Marambio L*, et al.* The Endoplasmic Reticulum Chaperone GRP78/BiP Modulates Prion Propagation in vitro and in vivo. *Scientific reports* 2017, **7:** 44723.
12. Evans CG, Chang L, Gestwicki JE. Heat shock protein 70 (hsp70) as an emerging drug target. *J Med Chem* 2010, **53**(12)**:** 4585-4602.
13. Li H, Xu W, Wu L, Dong B, Jin J, Han D*, et al.* Differential regulation of endoplasmic reticulum stress-induced autophagy and apoptosis in two strains of gibel carp (Carassius gibelio) exposed to acute waterborne cadmium. *Aquatic toxicology (Amsterdam, Netherlands)* 2021, **231:** 105721.
14. Liu MQ, Chen Z, Chen LX. Endoplasmic reticulum stress: a novel mechanism and therapeutic target for cardiovascular diseases. *Acta pharmacologica Sinica* 2016, **37**(4)**:** 425-443.
15. Beltramo E, Arroba AI, Mazzeo A, Valverde AM, Porta M. Imbalance between pro-apoptotic and pro-survival factors in human retinal pericytes in diabetic-like conditions. *Acta ophthalmologica* 2018, **96**(1)**:** e19-e26.
16. Shi M, Zhang H, Wang L, Zhu C, Sheng K, Du Y*, et al.* Premature Termination Codons Are Recognized in the Nucleus in A Reading-Frame Dependent Manner. *Cell discovery* 2015, **1:** 15001-.
17. Karamyshev AL, Karamysheva ZN. Lost in Translation: Ribosome-Associated mRNA and Protein Quality Controls. *Frontiers in genetics* 2018, **9:** 431.
18. Han X, Wei Y, Wang H, Wang F, Ju Z, Li T. Nonsense-mediated mRNA decay: a 'nonsense' pathway makes sense in stem cell biology. *Nucleic acids research* 2018, **46**(3)**:** 1038-1051.
19. Supek F, Lehner B, Lindeboom RGH. To NMD or Not To NMD: Nonsense-Mediated mRNA Decay in Cancer and Other Genetic Diseases. *Trends in genetics : TIG* 2021, **37**(7)**:** 657-668.
20. Nasif S, Contu L, Mühlemann O. Beyond quality control: The role of nonsense-mediated mRNA decay (NMD) in regulating gene expression. *Seminars in cell & developmental biology* 2018, **75:** 78-87.
21. Gupta P, Li YR. Upf proteins: highly conserved factors involved in nonsense mRNA mediated decay. *Molecular biology reports* 2018, **45**(1)**:** 39-55.
22. Karousis ED, Nasif S, Mühlemann O. Nonsense-mediated mRNA decay: novel mechanistic insights and biological impact. *Wiley interdisciplinary reviews RNA* 2016, **7**(5)**:** 661-682.
23. Li Z, Vuong JK, Zhang M, Stork C, Zheng S. Inhibition of nonsense-mediated RNA decay by ER stress. *RNA* 2017, **23**(3)**:** 378-394.
24. Tarpey PS, Raymond FL, Nguyen LS, Rodriguez J, Hackett A, Vandeleur L*, et al.* Mutations in UPF3B, a member of the nonsense-mediated mRNA decay complex, cause syndromic and nonsyndromic mental retardation. *Nat Genet* 2007, **39**(9)**:** 1127-1133.
25. Al-Jubran K, Wen J, Abdullahi A, Roy Chaudhury S, Li M, Ramanathan P*, et al.* Visualization of the joining of ribosomal subunits reveals the presence of 80S ribosomes in the nucleus. *RNA* 2013, **19**(12)**:** 1669-1683.

26. Tang X, Teder T, Samuelsson B, Haeggström JZ. The IRE1α Inhibitor KIRA6 Blocks Leukotriene Biosynthesis in Human Phagocytes. 2022, **13**.
27. Ghosh R, Wang L, Wang Eric S, Perera BGayani K, Igbaria A, Morita S*, et al.* Allosteric Inhibition of the IRE1α RNase Preserves Cell Viability and Function during Endoplasmic Reticulum Stress. *Cell* 2014, **158**(3)**:** 534-548.
28. Fribley AM, Miller JR, Reist TE, Callaghan MU, Kaufman RJ. Chapter Four - Large-Scale Analysis of UPR-Mediated Apoptosis in Human Cells. In: Conn PM (ed). *Methods in Enzymology*, vol. 491. Academic Press, 2011, pp 57-71.
29. Lee KP, Dey M, Neculai D, Cao C, Dever TE, Sicheri F. Structure of the dual enzyme Ire1 reveals the basis for catalysis and regulation in nonconventional RNA splicing. *Cell* 2008, **132**(1)**:** 89-100.
30. Sidrauski C, Walter P. The transmembrane kinase Ire1p is a site-specific endonuclease that initiates mRNA splicing in the unfolded protein response. *Cell* 1997, **90**(6)**:** 1031-1039.
31. Kadlec J, Izaurralde E, Cusack S. The structural basis for the interaction between nonsense-mediated mRNA decay factors UPF2 and UPF3. *Nature structural & molecular biology* 2004, **11**(4)**:** 330-337.
32. Wang H, Wang X, Ke ZJ, Comer AL, Xu M, Frank JA*, et al.* Tunicamycin-induced unfolded protein response in the developing mouse brain. *Toxicology and applied pharmacology* 2015, **283**(3)**:** 157-167.
33. Papandreou I, Denko NC, Olson M, Van Melckebeke H, Lust S, Tam A*, et al.* Identification of an Ire1alpha endonuclease specific inhibitor with cytotoxic activity against human multiple myeloma. *Blood* 2011, **117**(4)**:** 1311-1314.
34. Zhou J, Liu CY, Back SH, Clark RL, Peisach D, Xu Z*, et al.* The crystal structure of human IRE1 luminal domain reveals a conserved dimerization interface required for activation of the unfolded protein response. *Proc Natl Acad Sci U S A* 2006, **103**(39)**:** 14343-14348.
35. Tirasophon W, Welihinda AA, Kaufman RJ. A stress response pathway from the endoplasmic reticulum to the nucleus requires a novel bifunctional protein kinase/endoribonuclease (Ire1p) in mammalian cells. *Genes Dev* 1998, **12**(12)**:** 1812-1824.
36. Tirasophon W, Lee K, Callaghan B, Welihinda A, Kaufman RJ. The endoribonuclease activity of mammalian IRE1 autoregulates its mRNA and is required for the unfolded protein response. *Genes Dev* 2000, **14**(21)**:** 2725-2736.
37. Han X, Zhou J, Zhang P, Song F, Jiang R, Li M*, et al.* IRE1α dissociates with BiP and inhibits ER stress-mediated apoptosis in cartilage development. *Cellular signalling* 2013, **25**(11)**:** 2136-2146.
38. Clerici M, Deniaud A, Boehm V, Gehring NH, Schaffitzel C, Cusack S. Structural and functional analysis of the three MIF4G domains of nonsense-mediated decay factor UPF2. *Nucleic Acids Res* 2014, **42**(4)**:** 2673-2686.
39. Clerici M, Mourão A, Gutsche I, Gehring NH, Hentze MW, Kulozik A*, et al.* Unusual bipartite mode of interaction between the nonsense-mediated decay factors, UPF1 and UPF2. *EMBO J* 2009, **28**(15)**:** 2293-2306.

40. Belyy V, Tran NH, Walter P. Quantitative microscopy reveals dynamics and fate of clustered IRE1α. *Proc Natl Acad Sci U S A* 2020, **117**(3)**:** 1533-1542.
41. Koksal AR, Verne GN, Zhou Q. Endoplasmic reticulum stress in biological processing and disease. *J Investig Med* 2021, **69**(2)**:** 309-315.
42. Ariyasu D, Yoshida H, Hasegawa Y. Endoplasmic Reticulum (ER) Stress and Endocrine Disorders. *Int J Mol Sci* 2017, **18**(2).
43. Hetz CJNrMcb. The unfolded protein response: controlling cell fate decisions under ER stress and beyond. 2012, **13**(2)**:** 89-102.
44. Hetz C, Saxena SJNrN. ER stress and the unfolded protein response in neurodegeneration. 2017, **13**(8)**:** 477-491.
45. Kurosaki T, Popp MW, Maquat LE. Quality and quantity control of gene expression by nonsense-mediated mRNA decay. *Nat Rev Mol Cell Biol* 2019, **20**(7)**:** 406-420.
46. Chen C, Zhang X. IRE1α-XBP1 pathway promotes melanoma progression by regulating IL-6/STAT3 signaling. *J Transl Med* 2017, **15**(1)**:** 42.
47. Yoshida H, Matsui T, Yamamoto A, Okada T, Mori K. XBP1 mRNA is induced by ATF6 and spliced by IRE1 in response to ER stress to produce a highly active transcription factor. *Cell* 2001, **107**(7)**:** 881-891.
48. Park SM, Kang TI, So JS. Roles of XBP1s in Transcriptional Regulation of Target Genes. *Biomedicines* 2021, **9**(7).
49. Qiu Y, Mao T, Zhang Y, Shao M, You J, Ding Q*, et al.* A crucial role for RACK1 in the regulation of glucose-stimulated IRE1alpha activation in pancreatic beta cells. *Science signaling* 2010, **3**(106)**:** ra7.
50. Amin-Wetzel N, Saunders RA, Kamphuis MJ, Rato C, Preissler S, Harding HP*, et al.* A J-Protein Co-chaperone Recruits BiP to Monomerize IRE1 and Repress the Unfolded Protein Response. *Cell* 2017, **171**(7)**:** 1625-1637.e1613.
51. Li X, Sun S, Appathurai S, Sundaram A, Plumb R, Mariappan M. A Molecular Mechanism for Turning Off IRE1α Signaling during Endoplasmic Reticulum Stress. *Cell Rep* 2020, **33**(13)**:** 108563.
52. Wu IH, Yoon JS, Yang Q, Liu Y, Skach W, Thomas P. A role for the ribosome-associated complex in activation of the IRE1 branch of UPR. *Cell Rep* 2021, **35**(10)**:** 109217.
53. Li Y, Huang S, Wang J, Dai J, Cai J, Yan S*, et al.* Phosphorylation at Ser(724) of the ER stress sensor IRE1α governs its activation state and limits ER stress-induced hepatosteatosis. *J Biol Chem* 2022, **298**(6)**:** 101997.
54. Ricci D, Marrocco I, Blumenthal D, Dibos M, Eletto D, Vargas J*, et al.* Clustering of IRE1α depends on sensing ER stress but not on its RNase activity. *FASEB J* 2019, **33**(9)**:** 9811-9827.
55. Alrahbeni T, Sartor F, Anderson J, Miedzybrodzka Z, McCaig C, Müller B. Full UPF3B function is critical for neuronal differentiation of neural stem cells. *Mol Brain* 2015, **8:** 33.
56. Cabral-Miranda F, Hetz C. ER Stress and Neurodegenerative Disease: A Cause or Effect Relationship? *Curr Top Microbiol Immunol* 2018, **414:** 131-157.

57. Ghemrawi R, Khair M. Endoplasmic Reticulum Stress and Unfolded Protein Response in Neurodegenerative Diseases. *Int J Mol Sci* 2020, **21**(17).

58. Gorman A, Healy S, Jäger R, Samali AJP, therapeutics. Stress management at the ER: regulators of ER stress-induced apoptosis. 2012, **134**(3)**:** 306-316.

Figures

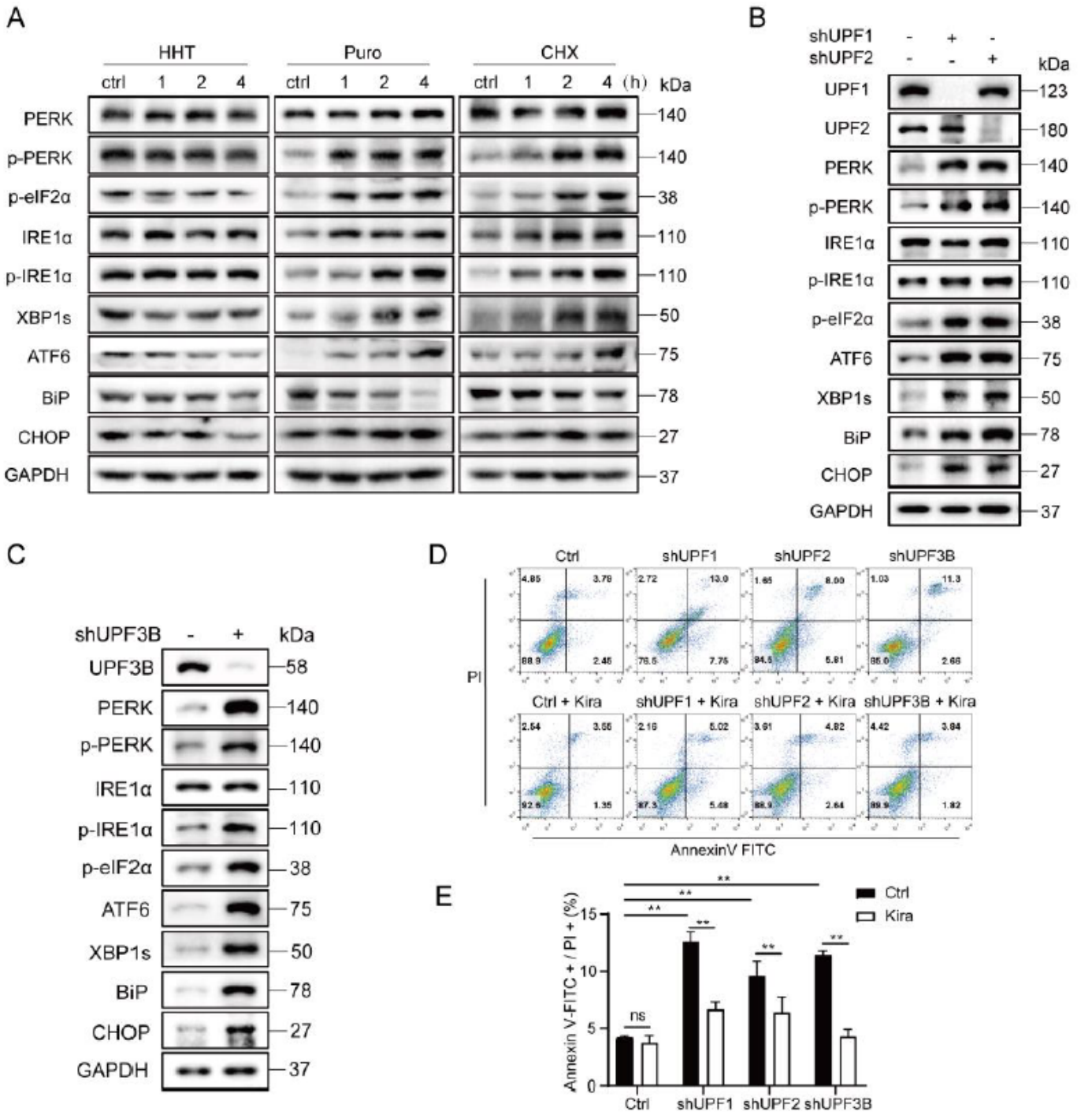

Figure 1

Translation inhibitor and knock down of NMD factors activate the UPR signaling pathway

(A) The expression of ER stress

related proteins w as evaluated under incubation with 2 μM harringtonine, with puromycin (100 μg/mL) and with cycloheximide (100 μg/mL) for 1 or 2 or 4 h. The cells were then harvested and subjected to western blotting analysis. (B C) UPF1, UPF2 and UPF3B were knocked down sta bly in HEK293T cells to detect the expression level of target proteins. All the target protein levels were analyzed by western blotting. (D) Flow cytometry analysis the apoptosis of shUPF cells with or without Kira6 treatment (50 μ M for 6 h). (E) Data stat istical 1 analyses were performed on Annexin V+/PI+ double positive cells in (D). The results are the means ± SEMs of at least three independent experiments. Statistical significance was defined as *p<0.05, **p<0.01 or ***p<0.001.

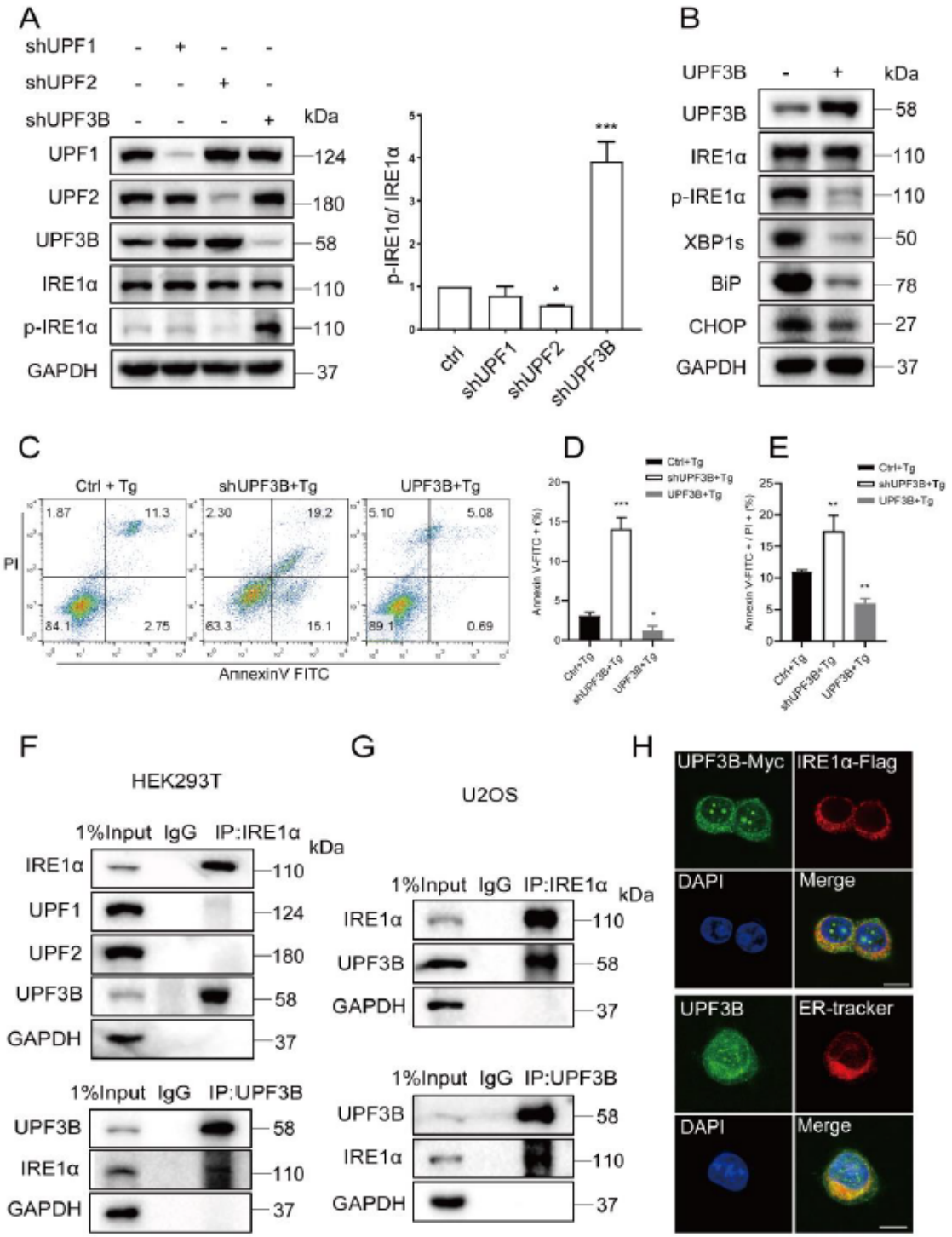

Figure 2

Unique regulation of UPF3B in activating the UPR signaling pathway

(A) The levels of phosphorylated IRE1

α were evaluated following treatment with shRNA of UPF1, UPF2 and UPF3B in HEK293T cells, respectively. The cells were then harvested and subjected to western blotting analysis, and the relative phosphorylation of IRE1 α were statistically analyzed by three independent experiments. *p<0.05, **p<0.01, ***p<0.001. (B) The expression of ER stress related proteins in UPF3B overexpression cells. HEK293T cells were transfected with pCMV or pCMV UPF3B for 24 h. The cells were then harvested and subjected to western blotting analysis. (C) Flow cytometry analysis apoptosis of shUPF3B and overexpression UPF3B cells under Tg (2 μ M for 3 h) treatment. (D E) Data stati stical analyses were performed on Annexin V+/PI+ double positive cells and Annexin V+ single positive cells in (C). (F G) UPF3B interacts with IRE1 α directly. Co IP analysis of the interaction between IRE1 α and UPF3B in HEK293T (F) and U2OS cells (G). The cells lysates were subjected to immunoprecipitation (IP) and western blot analysis with the indicated antibodies, IgG was used as a negative control in IP assay. (H) Up: the localization of IRE1 α and UPF3B was evaluated by an immunofluorescence assay. U2OS cells were fixed and stained with anti Flag antibody (red), anti Myc antibody (green) and DAPI (blue). Down: the localization of UPF3B and ER. U2OS cells were fixed and stained with anti UPF3B antibody (green), ER tracker (red) and DAPI (blue). Scale 10 μ m. The results are the means ± SEMs of at least three independent experiments. Statistical significance was defined as *p<0.05, **p<0.01 or ***p<0.001.

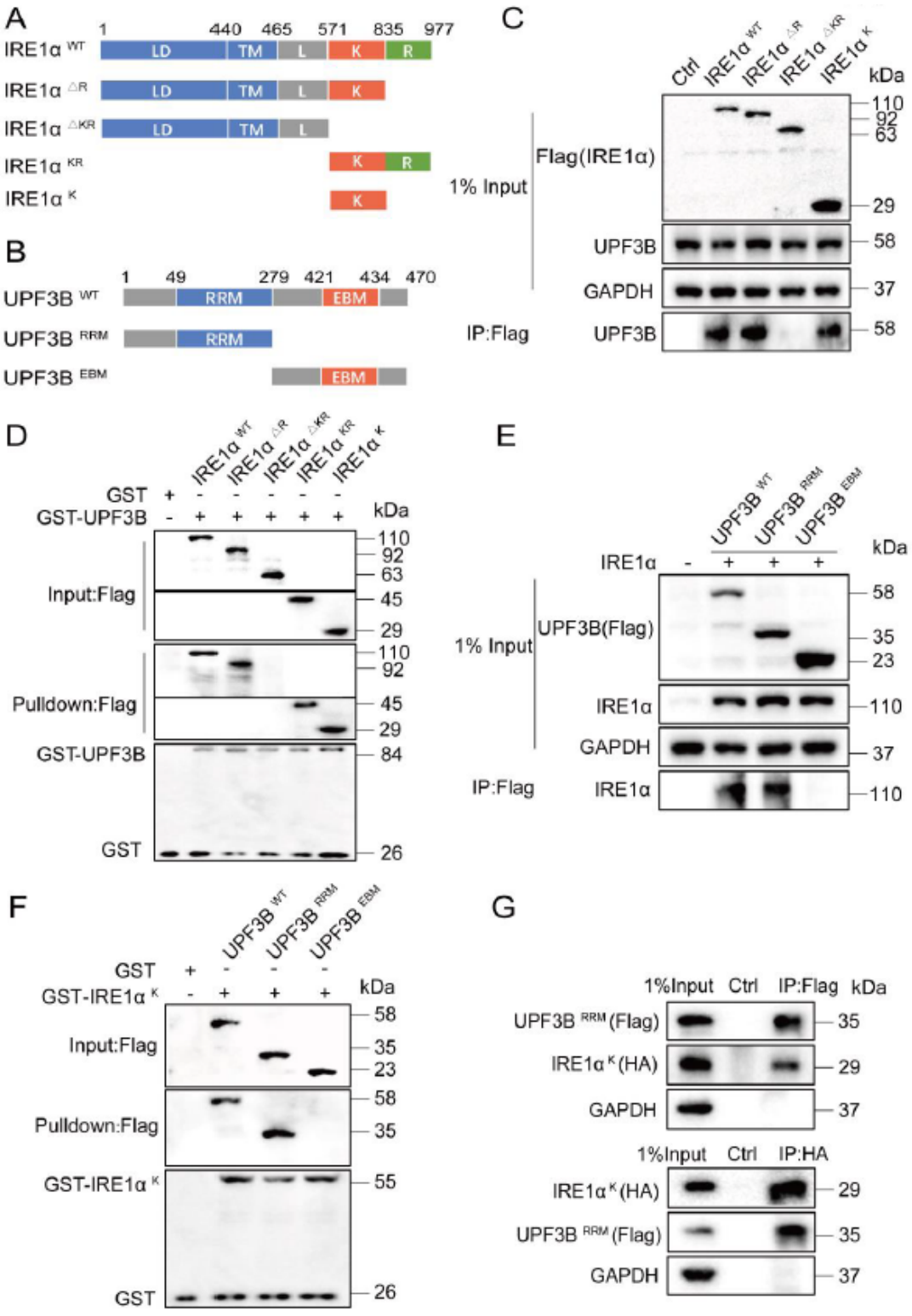

Figure 3

The kinase domain of IRE1

α interacts with the RRM domain of UPF3B

(A)

Diagram of the wild type (WT) and mutant versions of F lag tagged IRE1 α analyzed. The luminal domain (LD), transmembrane segment (TM), linker region (L), kinase (K), and RNase (R) domains are indicated. (B) Diagram of the wild type (WT) and mutant versions of F lag tagged

UPF3B analyzed. The RNA recognition motif (RRM)UPF3B analyzed. The RNA recognition motif (RRM) likelike domaindomain and exon junction complex and exon junction complex binding motif (EBM) are indicated. (C) Identification of the IRE1binding motif (EBM) are indicated. (C) Identification of the IRE1α α domain responsible for domain responsible for interacting with UPF3B. HEK293T cells were transfected with IRE1interacting with UPF3B. HEK293T cells were transfected with IRE1αα–Flag deletion mutants. The Flag deletion mutants. The cell lysates were immunoprecipitated with an anticell lysates were immunoprecipitated with an anti–Flag antibody, and the precipitates and wholeFlag antibody, and the precipitates and whole–cell lysates were then analyzed by western blotting. (D)cell lysates were then analyzed by western blotting. (D) The purified GST or GSTThe purified GST or GST–UPF3BUPF3B–fusion fusion protein bound to agarose beads was addprotein bound to agarose beads was added to the lysate of ed to the lysate of HEKHEK293T cells expressing 293T cells expressing IRE1IRE1αα–Flag Flag deletion mutantsdeletion mutants. After GST affinity purification, protein complexes were washed and detected by . After GST affinity purification, protein complexes were washed and detected by western blot analysis with antiwestern blot analysis with anti–FlagFlag or antior anti–GST as indicated. GST protein was used as a negative GST as indicated. GST protein was used as a negative contrcontrol.ol. ((EE)) Identification of the UPF3B domain responsible for interacting with IRE1Identification of the UPF3B domain responsible for interacting with IRE1α. α. Cells were Cells were transfected with IRE1transfected with IRE1α α and the two UPF3Band the two UPF3B–Flag deletion mutants. The cell lysates were Flag deletion mutants. The cell lysates were immunoprecipitated with an antiimmunoprecipitated with an anti–Flag antibody, and the precipitates and wholeFlag antibody, and the precipitates and whole–cell cell lysates were lysates were then analyzed by western blotting.then analyzed by western blotting. ((FF)) The purified GST or GSTThe purified GST or GST–IRE1IRE1ααKK–fusion protein bound to fusion protein bound to agarose beads was added to the lysate of agarose beads was added to the lysate of HEKHEK293T cells expressing 293T cells expressing UPF3BUPF3B–Flag deletion mutantsFlag deletion mutants. . After GST affinity purification, protein complexes werAfter GST affinity purification, protein complexes were washed and detected by western blot e washed and detected by western blot analysis with antianalysis with anti–FlagFlag or antior anti–GST as indicated. GST protein was used as a negative control.GST as indicated. GST protein was used as a negative control. ((GG)) The IRE1The IRE1α α kinase domain was interaction with UPF3B RRM kinase domain was interaction with UPF3B RRM likelike region. HEK293T cells were region. HEK293T cells were transfected with plasmids encodintransfected with plasmids encoding the indicated deletion mutants. The cell lysates were g the indicated deletion mutants. The cell lysates were immunoprecipitated with antiimmunoprecipitated with anti–Flag antibody and indicated antibodies, and the precipitates and Flag antibody and indicated antibodies, and the precipitates and whole cell lysates were then analyzed by western blotting.whole cell lysates were then analyzed by western blotting. The results are from three independent experiments.

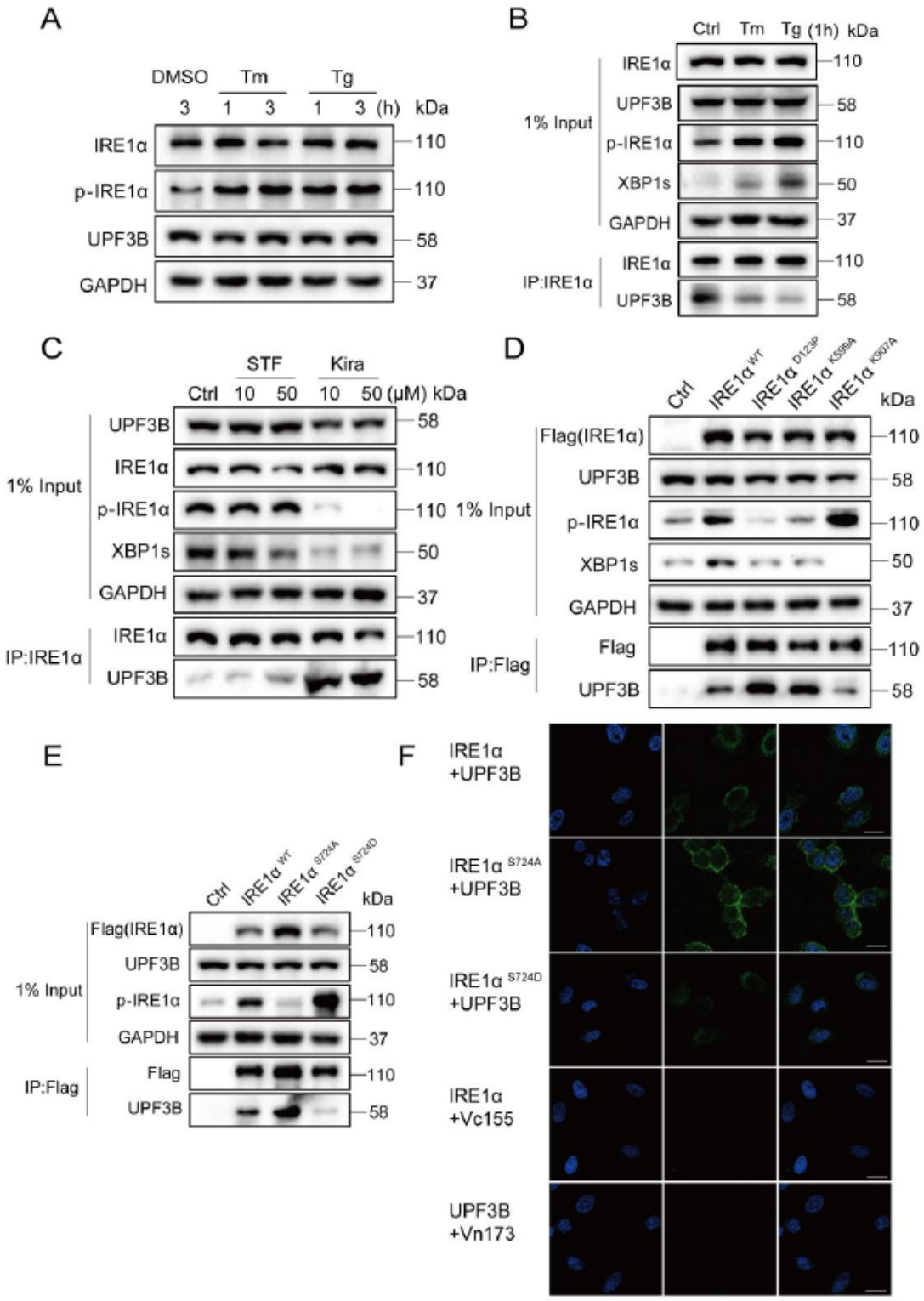

Figure 4

Phosphorylation of IRE1

α inhibit its interaction with UPF3B

(A) The levels of phosphorylated IRE1

α were evaluated following treatment with dimethyl sulfoxide (DMSO), Tg (2 μ M), or Tm (10 μ g/mL) for 1 or 3 h. All the target protein levels were analyzed by western blotting. (B) Immunoprecipitation analysis of the end ogenous interaction between IRE1 α and UPF3B under ER s tress . Cells were incubated with Tg and Tm for 1 h, and then subjected to western blotting analysis. (C) The effect of kinase and endonuclease activity of IRE1 α on the interaction between IRE1 α and UPF3 B. Cells were incubated with STF and Kira6 (10 or 50 μ M) for 6 h. The cell lysates were subjected to immunoprecipitation with the indicated antibodies, and visualized by western blotting. (D) Co IP analysis of the interaction between IRE1 α mutants and UPF3 B. HEK293T cells were transfected with the Flag tagged IRE1 α mutants for 24 h. The cell lysates were subjected to immunoprecipitation with the indicated antibodies, and visualized by western blotting. pCDNA3.1 transfection was used as a negative control. (E) Phosphorylation of IRE1 α inhibit the interaction between IRE1 α and UPF3B. HEK293T cells were transfected with IRE1 α WT , the IRE1 α S724 mutants for 24 h. The cells were then harvested and subjected to western blotting analysis. (F) The co localization of I RE1 α with UPF3B was evaluated by BiFC. IRE1 α VN173 and UPF3B VC155 constructs and the mutants were transfected into U2OS cells, then stained with Hoechst 33342. The figures show representative fluorescent images of the indicated proteins. Scale bar, 20 μ m. The results are the means ± SEMs of at least three independent experiments.

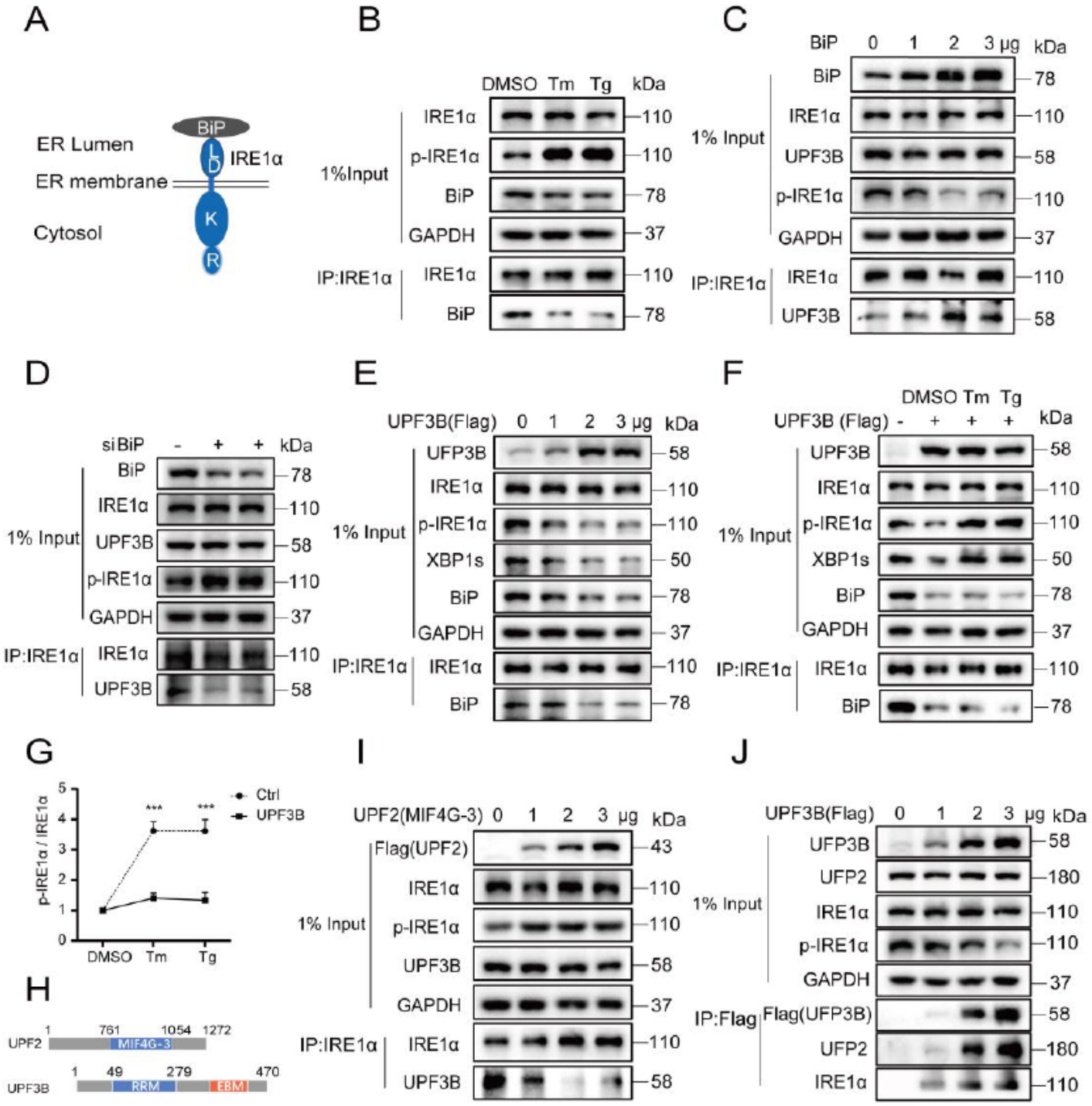

Figure 5

BiP and UPF3B jointly control the activation of IRE1 α

(A) Schematic diagram of the ER lumen domain of IRE1

α bound to BiP. (B) The interaction between IRE1α and BiP was inhibited during ER stress. Cells were incubated with Tg and Tm for 1 h, the cell lysates were subjected to immunoprecipitation with the indic ated antibodies and visualized by western blotting. (C) BiP enhances the interaction between IRE1α and

UPF3B. After 24h transient overexpression of BiP plasmid in HEK293T cell line, cells were collected and immunoprecipitation was performed with anti IRE1 α antibody for western blotting analysis. (D) siBiP inhibit the interactions of UPF3B and IRE1 α. After transfection of 20 nM BiP siRNA or negative control siRNA in HEK293T cell line, cells were collected 48 h later and immunoprecipitation with anti IRE1 α an tibody for Western blotting analysis. (E) Overexpression of UPF3B plasmid in HEK293T cell line, cells were collected and immunoprecipitation with anti IRE1 α antibody for western blotting analysis. (F) Overexpression of UPF3B and incubated with Tg (2 μ M) an d Tm (10 μ g/mL) for 1 h, cells were collected and immunoprecipitation with anti IRE1 α antibody for western blotting analysis. (G) Overexpression of UPF3B inhibited IRE1 α phosphorylation under ER stress. The data were from figure 5B and 5F. (H) Schematic diagram of the structural domains of UPF2 and UPF3B interactions. (I) UPF2 inhibits the interaction between UPF3B and IRE1 α by competing with UPF3B. After gradient overexpression of UPF2 MIF4G 3 plasmid in HEK293T cell line for 24 h, cells were c ollected and immunoprecipitation was performed with anti Flag antibody for western blotting analysis. (J) UPF3B interacts with UPF2 and IRE1 α in a dosage dependent manner. After gradient overexpression of UPF3B plasmid in HEK293T cell line for 24 h, cells were collected and immunoprecipitation was performed with anti Flag antibody for western blotting analysis. The results are the means ± SEMs of at least three independent experiments. Statistical significance was defined as *p<0.05, **p<0.01 or ***p<0.001.

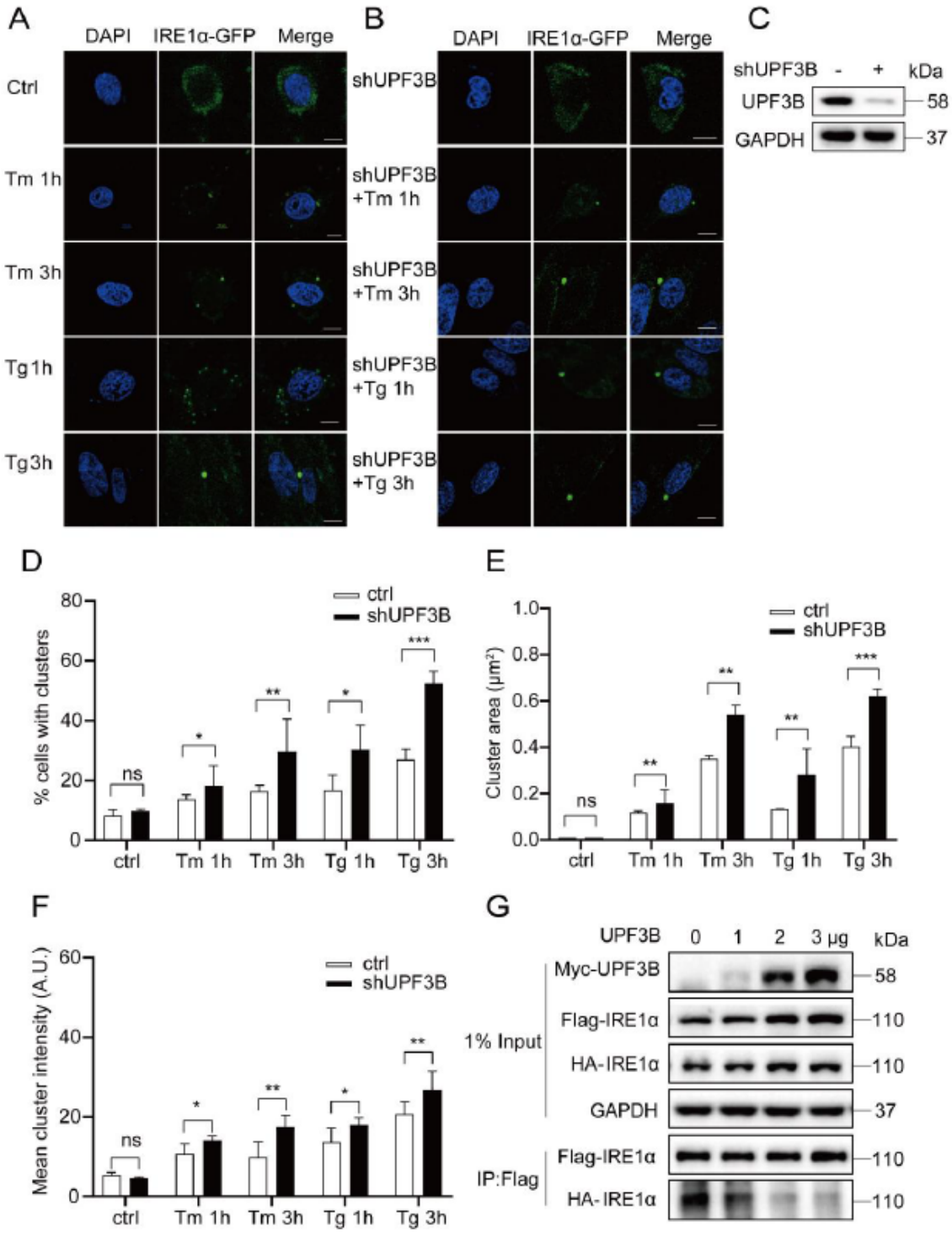

Figure 6

UPF3B inhibit the formation of IRE1α cluster under ER stress

(A-C) The IRE1α-GFP plasmid was overexpressed in U2OS cells for 24 h and treated with corresponding Tg (2 μ M) and Tm (10 μ g/mL) for 1 or 3 h. The cells were stained with Hoechst 33342. The scale is 10 μm. (D) Percentage of total cell fluorescence intensity found in clusters at each time point. (E)

Distribution of cluster sizes during the time course. (F) Distribution of cluster fluorescence intensities at each time point. Each dot represents 1 field, 5 fields were analyzed for each condition and an average of 60 cells were analyzed per condition in each experiment. (G) UPF3B inhibited IRE1α oligomerization. UPF3B-Myc, IRE1α-Flag and IRE1α-HA were overexpressed in HEK293T cells. Cells were collected and immunoprecipitation was performed with anti-Flag antibodies for western blotting analysis. The results are the means ± SEMs of at least three independent experiments. Statistical significance was defined as *p<0.05, **p<0.01 or ***p<0.001.

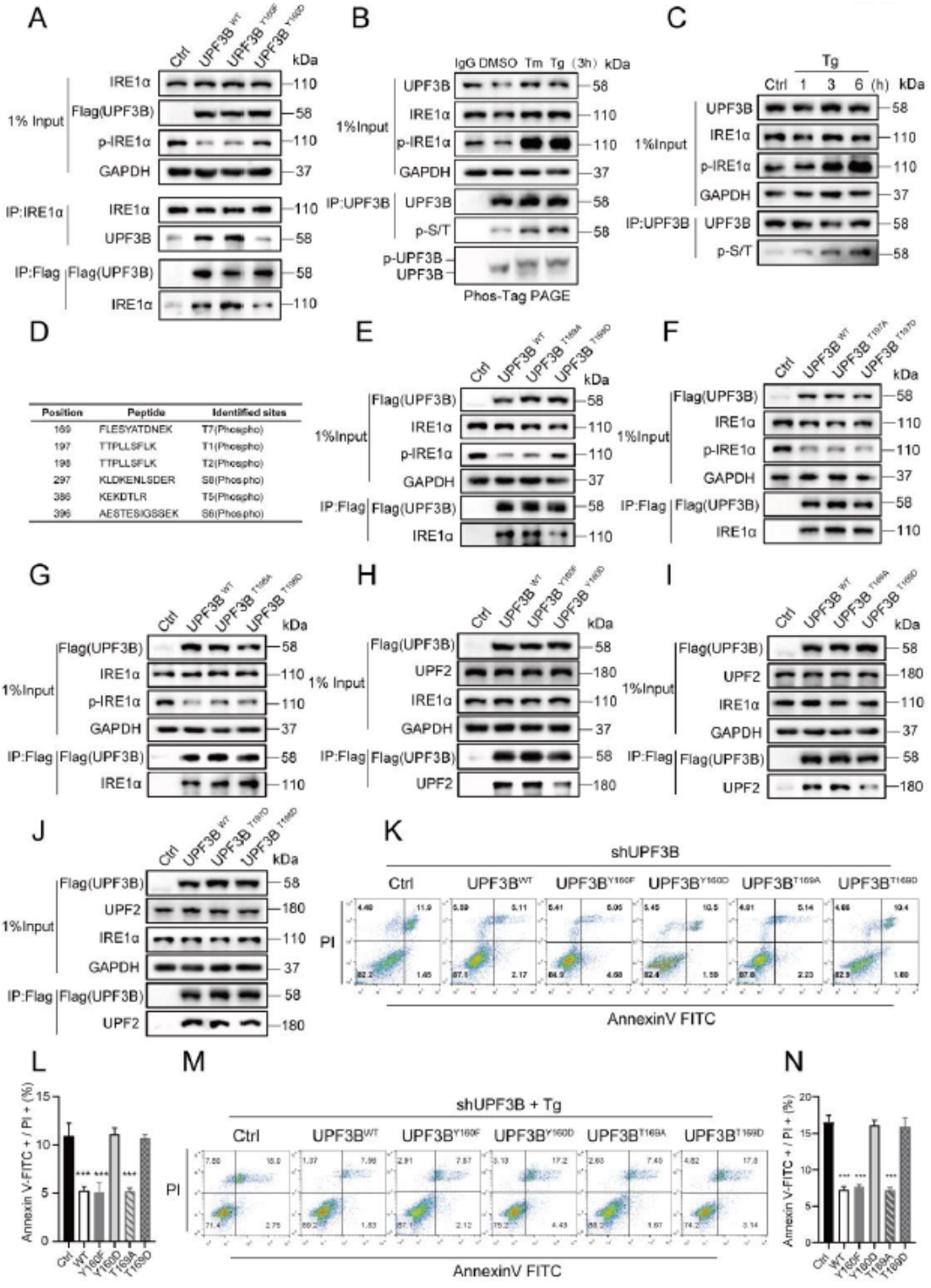

Figure 7

The UPF3B can be phosphorylated during ER stress

(A)

HEK293T cells were transfected with UPF3B WT , the UPF3B Y160F mutant, or the UPF3B Y160D mutant for 24 h. Cell lysates were subjected to immunoprecipitation with the Flag or IRE1α antibodies and visualized by western blotting. (The expression levels of phosphorylated threonine and serine of UPF3B were evaluated following treatment with Tg (2 μ M) and Tm (10 μ g/mL) for 3 h. Cell lysates were subjected to immunoprecipitation with the UPF3B antibodies, and visualized by western blotting (The expression levels of phosphorylated UPF3B were evaluated following treatment with T g for 1,3 or 6 h. D Phosphorylation mapping mass spectrometry of human UPF3B from cells. HEK293T cells were evaluated following treatment with Tg (2 μ M) for 6 h. Cell lysates were subjected to immunoprecipitation with the UPF3B antibodies and i dentification by mass spectrometry E Analysis of the interaction between IRE1α and UPF3B nts . HEK293T cells were transfected with UPF3B WT , the UPF3B T 16 9A mutant, or the UPF3B T169D mutant for 24 h. T he cells were harvested for immunoprecipitation with antibodies against Flag . F G Analysis of the interaction between IRE1α and UPF3B mutants . Cells were transfected with UPF3B mutants for 24 h and then harvested for immunoprecipitation with antibodies against Flag. H J Analysis of the interaction between UPF 2 and UPF3B mutants . Cells were transfected with UPF3B mutants for 24 h and then harvested for immunoprecipitation with antibodies against Flag K , M Flow cyto metry analysis of apoptotic changes by supplemented with different UPF3B mutants in physiological o r under Tg (2 μ M for 3 h) treatment in sh UPF3B cell lines . L , N) Data statistical analyses were performed on Annexin V+/PI+ double positive cells in (K) and (The results are the means ± SEMs of at least three independent experiments. Statistical significance was defined as *p<0.05, **p<0.01 or ***p<0.001.

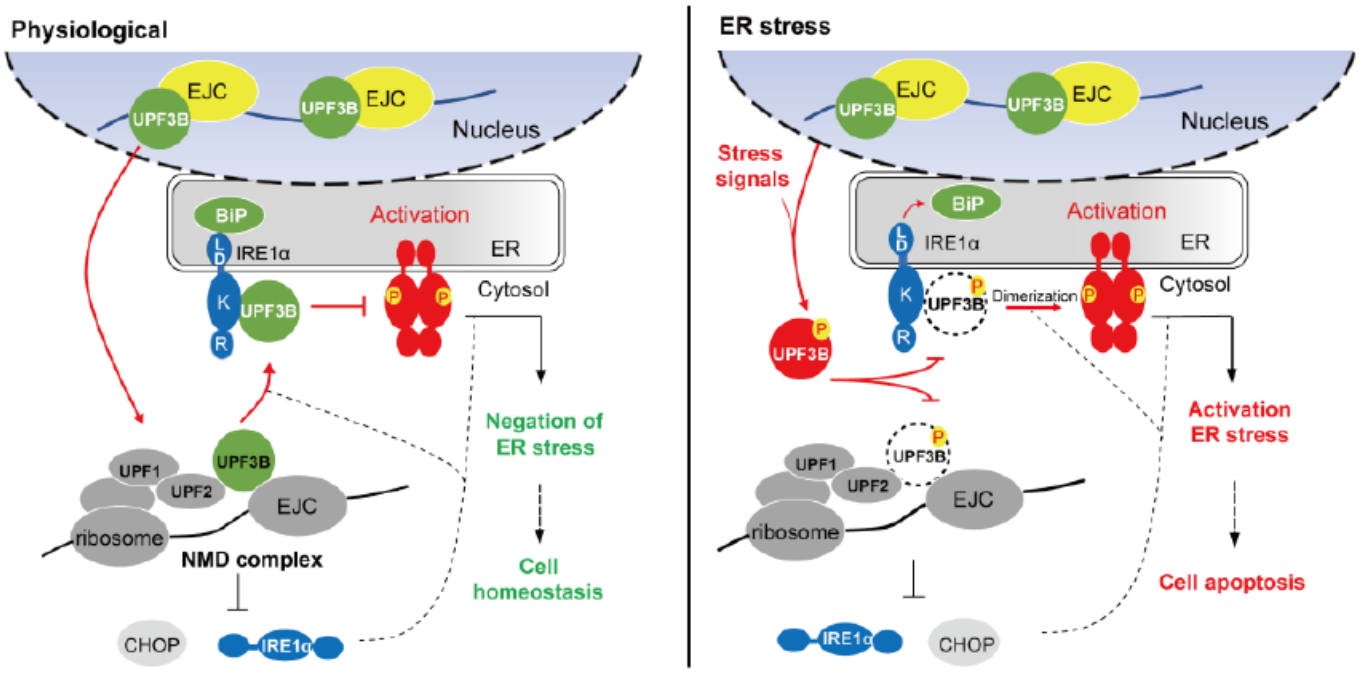

Figure 8

The dual role of UPF3B in NMD and ER stress

Under physiological conditions, UPF3B inhibits the activation of IRE1

α and affects its phosphorylation and oligomerization by interacting with the IRE1 α kinase domain. UPF3B and BiP jointly control the activation of IRE1 α. In addition, NMD can inhibit ER s tress by control the expression of IRE1 α and CHOP, and negatively feedback ER stress to reshape cell homeostasis. During ER stress, UPF3B is phosphorylated and dissociates from IRE1 α, which promotes the expression of IRE1 α and CHOP, and activates ER stress , leading to

Supplementary Files

This is a list of supplementary files associated with this preprint. Click to download.

- Supplementaldata.pdf